Modelling the Cortical Columnar Organisation for Topological State-Space Representation, and Action Planning

Louis-Emmanuel Martinet[1,2,3], Benjamin Fouque[1,2,3], Jean-Baptiste Passot[2,3], Jean-Arcady Meyer[1], and Angelo Arleo[2,3]

[1] Université Pierre et Marie Curie - Paris 6, FRE2507, ISIR, Paris, F-75016, France
[2] UPMC Univ Paris 6, UMR 7102, F-75005, Paris, France
[3] CNRS, UMR 7102, F-75005, Paris, France
louis-emmanuel.martinet@isir.fr

Abstract. We present a neuromimetic navigation system modelling the columnar structure of the cortex to mediate spatial learning and action planning. The model has been validated on a spatial behavioural task, namely the Tolman & Honzik's *detour* protocol, which allowed us to test the ability of the system to build a topological representation of the environment, and to use it to exhibit flexible goal-directed behaviour (i.e., to predict the outcome of alternative trajectories to avoid blocked pathways). First, it is shown that the model successfully reproduces the navigation performance of rodents in terms of goal-directed path selection. Second, we report on the neural response patterns characterising the learnt columnar space representation.

1 Introduction

This paper presents a biomimetic model of action planning inspired by the columnar organisation of the mammalian neocortex. Planning is defined here as the ability, given a state space S and an action space A, to "mentally" explore the $S \times A$ space to infer an appropriate sequence of actions leading to a goal state $s_g \in S$. This definition calls upon the capability of *(i)* predicting the consequences of actions, i.e. the most likely state $s' \in S$ to be reached when an action $a \in A$ is executed from a state $s \in S$, *(ii)* evaluating the effectiveness of the selected plan on-line. The model generates a topological representation of the environment, and it employs an activation-diffusion mechanism to plan goal-directed trajectories. The activation-diffusion process is based on the propagation of a reward-dependent activity signal from the goal state s_g through the entire topological network. This propagation process enables the system to generate sequences of actions (i.e., trajectories) from the current state s towards s_g.

Topological map learning and path planning have extensively been studied in biomimetic robotics [1]. We focus on models inspired by the anatomical organisation of the cortex, and implementing an activation-diffusion planning principle. The existence of cortical columns was first reported by Mountcastle [2], who observed vertical groups of neurones responding to the same external stimuli simultaneously. Neuroanatomical findings suggest that these "functional columns" can be further divided into several "minicolumns", i.e. vertical bundles of neurones across the layers of the cortex separated from each other by a cell-poor area [3].

Burnod [4] proposed one of the first models of the cortical column architecture, called "cortical automaton". He also described a "call tree" process that can be seen as a neuromimetic implementation of the activation-diffusion principle. Several action selection models were inspired by Burnod's hypothesis. Some of these works employed the cortical automaton concept explicitly [5–7]. Others used either more classical connectionist architectures [8–10] or Markov decision processes [11]. Yet, none of these works took into account the multilevel coding property offered by the possibility to refine the cortical organisation by adding a sublevel to the column, i.e. the minicolumn. The topological representation presented here exploits this idea by associating the columnar level to a compact representation of the environment, and by employing the minicolumn level to characterise the agent's behaviour.

In order to validate the preliminary version of the model, we have implemented it on a simulated robot, and tested it on the classical navigation task designed by Tolman & Honzik [12]. This protocol allowed us to assess the ability of the system to learn topological representations, and to exploit them to perform flexible goal-directed behaviour (e.g., planning optimal *detour* trajectories). The Tolman & Honzik's task is a purely spatial navigation protocol. Our middle-term goal is to extend the cortical model presented here to elaborate more abstract contextual representations. For example, besides learning the spatial properties of the environment, the system shall be able to encode multidimensional information, such as motivation-dependent memories, multiscale spatio-temporal correlates, and action cost/risk constraints.

2 Methods

2.1 Single neurone model

The elementary computational units of the model are artificial firing-rate neurones i, whose mean discharge $r_i \in [0, 1]$ is given by:

$$r_i(t) = f\Big(V_i(t) \cdot (1 \pm \epsilon)\Big) \tag{1}$$

where $V_i(t)$ is the membrane potential at time t, f is the transfer function, and ϵ is a random noise uniformly drawn from $[0, 0.01]$. The potential V_i varies according to:

$$\tau_i \cdot \frac{dV_i(t)}{dt} = -V_i(t) + I_i(t) \tag{2}$$

where $\tau_i = 10$ ms is the membrane time constant, and $I_i(t)$ is the synaptic drive generated by all the afferent inputs at time t. Eq. 2 is integrated by using a time step $\Delta_t = 1$ ms. Both the synaptic drive $I_i(t)$ and the transfer function f are characteristic of the different types of model units, and they will be defined thereafter.

2.2 Encoding space and actions: the minicolumn and column model

The main inputs to the cortical model are the location- and orientation-selective activities of hippocampal place (HP) and head-direction cells, respectively [13, 14]. The HP field representation is built incrementally as the animat explores the environment, and it provides the system with a continuous distributed and redundant state representation S [15, 16]. A major objective of the cortical model is to build a more compact state-action representation $S \times A$ suitable for topological map learning and action planning.

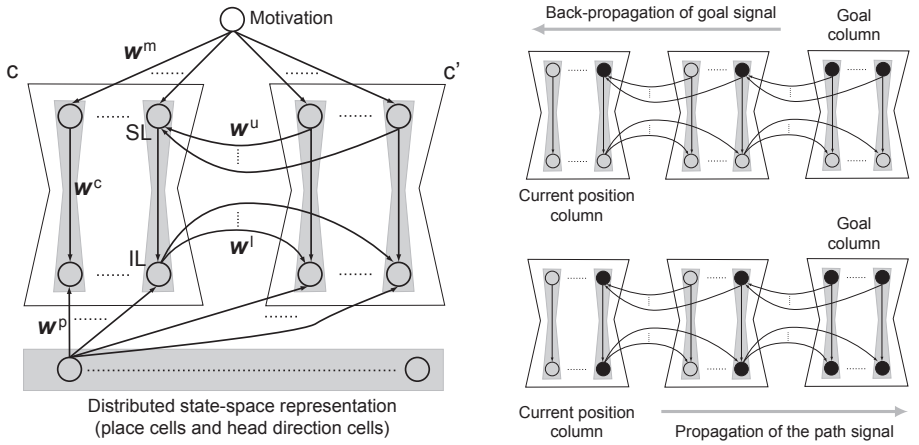

Fig. 1. The cortical model and the activation-diffusion process. **(A)** The architecture of two column units c and c'. Columns are composed of sets of minicolumns (vertical grey regions), each of which consists of a supragranular layer unit (SL) and an infragranular layer unit (IL). **(B)** Top: back-propagation of the motivational signal through the network of SL neurones. Bottom: forward-propagation of the goal-directed action signal through the IL neurones.

In the model, the basic component of the columnar organisation is the minicolumn (vertical grey regions in Fig. 1). An unsupervised learning scheme (see Sec. 2.3) is employed to make the activity of each minicolumn selective to a specific state-action pair $(s, a) \in S \times A$. Notice that a given action $a \in A$ represents the allocentric motion direction of the animat when it performs the transition between two locations $s, s' \in S$. According to the learning algorithm, all the minicolumns selective for the same spatial location $s \in S$ are grouped to form a higher-level computational unit, i.e. the column (see c and c' in Fig. 1A). This architecture is inspired by biological data showing that minicolumns inside a column have similar selectivity properties [17]. Thus, columns consist of a set of minicolumns that are incrementally recruited to encode all the state-action pairs $(s, a_{1\ldots N}) \in S \times A$ experienced by the animat at a location s. During planning (see Sec. 2.4), all the minicolumns of a column compete with each other to locally infer the most appropriate goal-directed action.

Every minicolumn of the model consists of two computational units, representing supragranular layer (SL) and infragranular layer (IL) neurones (Fig. 1A). The discharge of SL and IL units simulates the mean firing activity of a population of cortical neurones in layers II-III, and V-VI, respectively. Each minicolumn receives three different sets of afferent projections (Fig. 1A): *(i)* Hippocampal inputs conveying space coding activity converge onto IL neurones; these connections are plastic, and their synaptic efficacy is determined by the weight distribution $\boldsymbol{w}^p$ (all the synaptic weights of the model are within the maximum range of $[0, 1]$). *(ii)* Collateral afferents from adjacent cortical columns converge onto the SL and IL neurones via the projections $\boldsymbol{w}^u$ and $\boldsymbol{w}^l$, respectively. These lateral connections are learnt incrementally (see Sec. 2.3), and

play a prominent role in both encoding the environment topology and implementing the activation-diffusion planning mechanism. *(iii)* SL neurones receive projections $\boldsymbol{w}^m$ conveying motivation-dependent signals. As shown in Sec. 2.4, this input is employed to relate the activity of a minicolumn to goal locations.

SL neurones discharge as a function of the motivational signals conveyed via both $\boldsymbol{w}^u$ and $\boldsymbol{w}^m$ inputs. The synaptic drive $I_i(t)$ depolarising a SL neurone i that belongs to a column c is given by:

$$I_i(t) = \max_{i' \in c' \neq c} \left\{ w^u_{ii'} \cdot r_{i'}(t) \right\} + w^m_i \cdot r_m \tag{3}$$

where i' indexes other SL neurones of the cortical network; w^m_i and r_m are the weight and the intensity of the motivational signal, respectively. In the current version of the model the motivational input is generated algorithmically, i.e. $w^m_i = 1$ if column c is associated to the goal location, $w^m_i = 0$ otherwise, and the motivational signal $r_m = 1$. The membrane potential of unit i is then computed according to Eq. 2, and its firing rate $r_i(t)$ is obtained by means of an identity transfer function f.

Within each minicolumn, SL neurones project onto IL units via non-plastic projections $\boldsymbol{w}^c$ (Fig. 1A). Thus, IL neurones are driven by HP cells p (via the projections $\boldsymbol{w}^p$), by IL neurones belonging to adjacent columns (via the collaterals $\boldsymbol{w}^l$), and by SL units i (via $\boldsymbol{w}^c$). The synaptic drive of a IL neurone $j \in c$ is:

$$I_j(t) = \max\Big\{ \sum_{p \in HP} w^p_{jp} \cdot r_p(t) \ , \ \max_{j' \in c' \neq c} \left\{ w^l_{jj'} \cdot r_{j'}(t) \right\} \Big\} + w^c_{ji} \cdot r_i(t) \tag{4}$$

where j' indicates other IL neurones of the network; $w^c_{ji} = 1$ if the SL neurone i and the IL neurone j belong to the same minicolumn, $w^c_{ji} = 0$ otherwise. Then, the membrane potential $V_j(t)$ is computed by Eq. 2, and a sigmoidal transfer function f is employed to calculate $r_j(t)$. The parameters of the transfer function change online to adapt the electroresponsiveness properties of IL neurones j to the strength of their inputs [18].

2.3 Unsupervised growing network scheme for topological map learning

The topological representation is built incrementally as the animat explores the environment. At each location visited by the agent at time t the cortical network is updated if-and-only-if the infragranular layers of all existing minicolumns remain silent, i.e. $\sum_j \mathcal{H}(r_j(t) - \rho) = 0$, where j indexes all the IL neurones, $\mathcal{H}$ is the Heaviside function (i.e., $\mathcal{H}(x) = 1$ if $x \geq 0$, $\mathcal{H}(x) = 0$ otherwise), and $\rho = 0.1$. If at time t the novelty condition holds, a new group of minicolumns (i.e., a new column c) is recruited to become selective to the new place. Then, all the simultaneously active place cells $p \in HP$ are connected to the new IL units $j \in c$. Weights w^p_{jp} are initialised according to: $w^p_{jp} = \mathcal{H}(r_p - \rho) \cdot r_p$. For $t' > t$, the synaptic strength of these connections is changed by unsupervised Hebbian learning combined to a winner-take-all scheme. Let c be the column selective for the position visited by the animat at time t', i.e. let all the $j \in c$ be the most active IL units of the network at time t'. Then:

$$\Delta w^p_{jp} = \eta \cdot r_p \cdot (r_j - w^p_{jp}) \tag{5}$$

with $\eta = 0.005$. Whenever a state transition occurs, the collateral projections $\boldsymbol{w}^l$ and $\boldsymbol{w}^u$ are updated to relate the minicolumn activity to the state-action space $S \times A$. For instance, let columns c and c' denote the animat position before and after a state transition,

respectively (Fig. 1A). A minicolumn $\theta \in c$ becomes selective for the locomotion orientation taken by the animat to perform the transition. A new set of projections $w^l_{j'j}$ are then established from the IL unit $j \in \theta$ of column c to all the IL units j' of the column c'. In addition, at the supragranular level, a new set of connections $w^u_{ii'}$ is learnt to connect all the SL units of column c', i.e. $i' \in c'$, to the SL unit i of the minicolumn $\theta \in c$. The strengths of the lateral projections are initialised as: $w^l_{j'j} = w^u_{ii'} = \beta_{LTP},\ \forall i', j' \in c'$, with $\beta_{LTP} = 0.9$. Finally, in order to adapt the topological representation online, a synaptic potentiation-depression mechanism can modify the lateral projections $\boldsymbol{w}^l$ and $\boldsymbol{w}^u$. For example, if a new obstacle prevents the animat from achieving a previously learnt transition from column c to c' (i.e., if the activation of the IL unit $j \in \theta \in c$ is not followed in the time by the activation of all IL units $j' \in c'$), then a depression of the $w^l_{j'j}$ synaptic efficacy occurs: $\Delta w^l_{j'j} = -\beta_{LTD} \cdot w^l_{j'j},\ \forall j' \in c'$, where $\beta_{LTD} = 0.5$. The projections $w^u_{ii'}$ are updated similarly. A compensatory potentiation mechanism reinforces both $\boldsymbol{w}^l$ and $\boldsymbol{w}^u$ connections whenever a previously experienced transition is performed successfully: $\Delta w^l_{j'j} = \beta_{LTP} - w^l_{j'j},\ \forall j' \in c'$. The weights $w^u_{ii'}$ are updated similarly. Notice that $\boldsymbol{w}^l, \boldsymbol{w}^u \in [0, \beta_{LTP}]$.

2.4 Action planning

This model aims at developing a high-level controller determining the agent's behaviour based on action planning. Yet, a low-level reactive module enables the animat to avoid obstacles. Whenever the proximity sensors detect an obstacle, the reactive module takes control and prevents collisions. Also, the simulated animal behaves in order to either follow planned pathways (i.e., exploitation) or improve the topological map (i.e., exploration). This exploitation-exploration tradeoff is governed by an ϵ-greedy selection mechanism, with $\epsilon \in [0, 1]$ decreasing exponentially over time [16].

Fig. 1B shows an example of activation-diffusion process mediated by the columnar network. During trajectory planning, the SL neurones of the column corresponding to the goal location s_g are activated via a motivational signal r_m (see Eq. 3). Then, the SL activity is back-propagated through the network by means of the lateral projections $\boldsymbol{w}^u$ (Fig. 1B, top). During planning, the responsiveness of IL neurones (Eq. 4) is decreased to detect coincident inputs. In particular, the occurrence of the SL input r_i is a necessary condition for a IL neurone j to fire. In the presence of the SL input r_i, either the hippocampal signal r_p or the intercolumn signal r'_j are sufficient to activate the IL unit j. When the back-propagated goal signal reaches the minicolumns selective for the current position s this coincidence event occurs, which triggers the forward propagation of a goal-directed path signal through the projections $\boldsymbol{w}^l$ (Fig. 1B, bottom).

Goal-directed trajectories are generated by reading out the successive activations of IL neurones. Action selection calls upon a competition between the minicolumns encoding the $(s, a_{1\ldots N}) \in S \times A$ pairs, where s is the current location, and $a_{1\ldots N}$ are the transitions from s to adjacent positions s'. For sake of robustness, competition occurs over a 10-timestep cycle. It is worth stressing that each SL synaptic relay attenuates the goal signal by a factor $w^u_{ii'}$ (Eq. 3). That is, the smaller the number of synaptic relays, the stronger the goal signal received by the SL neurone corresponding to the current location s. Because the model column receptive fields are distributed rather uniformly over the environment, the intensity of the goal signal at a given location s is correlated to the distance between s and the target position s_g.

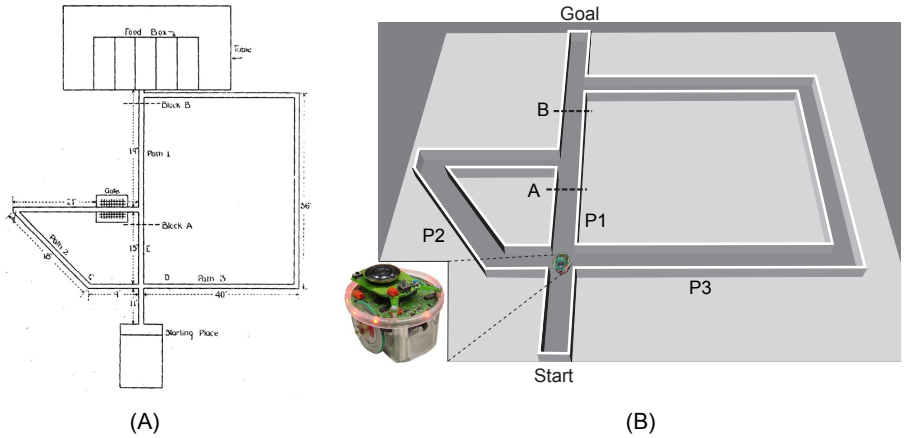

Fig. 2. (A) Tolman & Honzik's maze [12]. The gate near the second intersection allowed the rats to go from left to right only. **(B)** The simulated maze and robot. The dimensions of the simulated maze were taken so as to maintain the proportions of the real Tolman & Honzik's experimental setup. Bottom-left inset: the real *e-puck* mobile robot has a diameter of 70 mm and is 55 mm tall.

2.5 The behavioural task and the animat

In order to validate our navigation planning system, we chose the classical experimental task proposed by Tolman & Honzik [12]. The main objective of this behavioural protocol was to demonstrate that rodents undergoing a navigation test are able to show some "insights", e.g. to predict the outcome of alternative trajectories leading to a goal location in the presence of blocked pathways. The original Tolman & Honzik's maze is shown in Fig. 2A. It consisted of three narrow alleys of different lengths (Paths 1, 2, and 3) guiding the animals from a starting position (bottom) to a feeder location (top).

We implemented our model by means of the Webots© robotics simulation software. Fig. 2B shows a simulated version of the Tolman & Honzik's apparatus, and the simulated robot. We emulated the experimental protocol designed by Tolman & Honzik to assess the subjects' navigation performance. The overall protocol consisted of a training period followed by a probe test. Both training and probe trials were stopped when the subject had found the goal.

Training period: it lasted 14 days with 12 trials per day. The subjects could explore the maze and learn a navigation policy by developing their preferences for P1, P2, and P3.

- During Day 1, a series of 3 *forced runs* was carried out, in which additional doors were used to force the subjects to go successively through P1, P2, and P3. Then, during the remaining 9 runs, all additional doors were removed, and the subjects could explore the maze freely. At the end of the first training day, a preference for P1 was expected to be already developed [12].
- From Day 2 to 14, a block was introduced at place A (Fig. 2B) to require a choice between P2 and P3. In fact, additional doors were used to close the entrances to P2 and P3 to force subjects to go first to the Block A. Then, doors were removed, and subjects were forced to decide between P2 and P3 on their way back to the

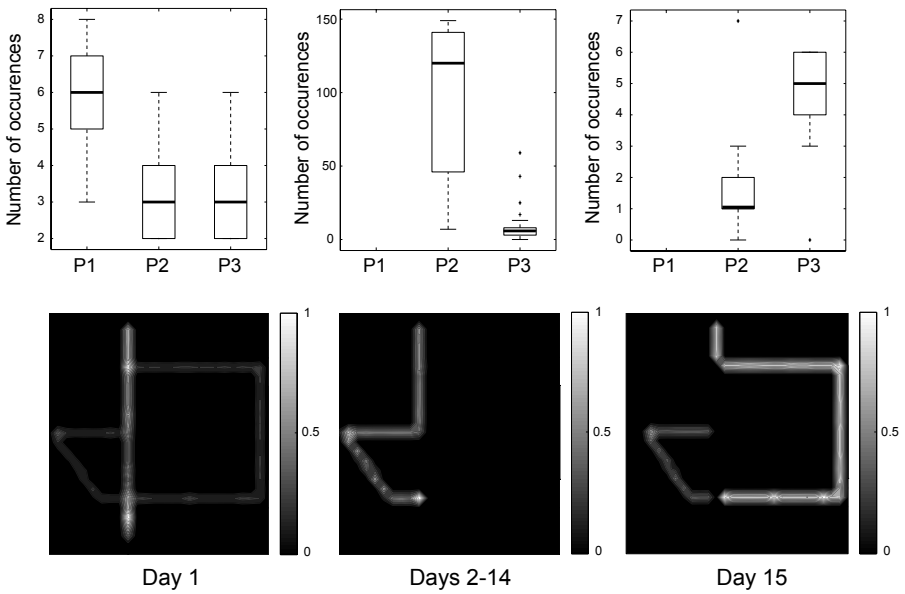

Fig. 3. Behavioural results. **Top row:** mean number of transits through P1, P2, and P3 (averaged over 100 experiments). **Bottom row:** occupancy grid maps.

first intersection. Each day, there were 10 "Block at A" runs that were mixed with 2 non-successive free runs to maintain the preference for P1.

Probe test period: it lasted 1 day (Day 15), and it consisted of 7 runs during which a block was placed at position B to interrupt the common section (Fig. 2B). The subjects were forced to decide between P2 and P3 when returning to the first intersection point.

For these experiments, Tolman & Honzik used 10 male rats of mixed breed, from 5 to 8 months old, with no previous training. In our simulations, we used a population of 100 animats, and we assessed the statistical significance of the results by means of an ANOVA analysis (the significant threshold was set at 10^{-2}, i.e. $p < 0.01$ was considered significant).

3 Results

3.1 Behavioural analysis

Day 1. During the first 12 training trials, the animats learnt the maze topology, and planned their trajectory in the absence of both block A and B (Fig. 2B). Similar to Tolman & Honzik's findings, our results show that the model learnt to select the shortest pathway P1 significantly more frequently than the alternative paths P2, P3 (ANOVA, $F_{2,297} = 168.249$, $p < 0.0001$). The quantitative and qualitative analyses reported on Fig. 3 (left) describe the path selection performance averaged over 100 experiments.

Days 2-14. During this training phase (consisting of 156 trials), a block was introduced at location A (Fig. 2B), which forced the animats to update their topological

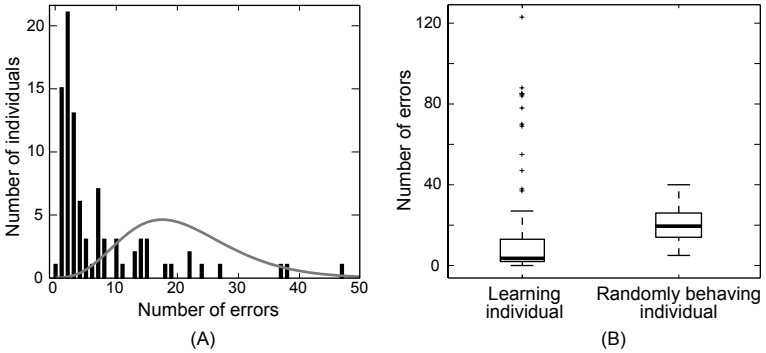

Fig. 4. Comparison between a learning and a randomly behaving agent. **(A)** Error distribution of learning (black histogram) versus random (grey line) animats. **(B)** Boxplots of the number of errors done on average by our model and by a randomly behaving agent.

maps dynamically, and to plan a *detour* to the goal. The results reported by Tolman & Honzik provided strong evidence for a preference for the shortest *detour* path P2. Consistently, in our simulations (Fig. 3, centre) we observed a significantly larger number of transits through P2 compared to P3 (ANOVA, $F_{1,198} = 383.068$ $p < 0.0001$), P1 being ignored in this analysis (similar to Tolman & Honzik's analysis) because blocked.

Day 15. In agreement with Tolman & Honzik's protocol, seven probe trials were performed during the 15th day of the simulated protocol, by removing the block A and adding a new block B (Fig. 2B). This manipulation aimed at testing the "insight" working hypothesis: after a first run through the shortest path P1 and after having encountered the unexpected block B, will rats try P2 or will they go directly through P3? According to Tolman & Honzik's results, the rats behaved as predicted by the insight hypothesis, i.e. they tended to select the longer but effective P3. The authors concluded that rats were able to inhibit the previously learnt policy (i.e., the "habit behaviour" consisting of selecting P2 after a failure of P1 during the 156 previous trials). Our probe test results are shown in Fig. 3 (right). Similar to rats, the animats exhibited a significant preference for P3 compared to P2 (ANOVA, $F_{1,198} = 130.15$, $p < 0.0001$). Finally, in order to further assess the mean performance of the system during the probe trials, we compared the action selection policy of learning animats with that of randomly behaving (theoretical) animats. Fig. 4A provides the results of this comparison by showing the error distribution over the population of learning agents (black histogram) and randomly behaving agents (grey curve). The number of errors per individual are displayed in the boxplot of Fig. 4B. These findings indicate a significantly better performance of learning animats compared to random agents (ANOVA, $F_{1,196} = 7.4432$, $p < 0.01$).

3.2 Analysis of neural activities

A series of additional analyses were done to begin to characterise the underlying processes (e.g., neural activities) subserving the action selection behaviour of the model. We measured the mean spatial density of the receptive fields of HP cells and cortical column units of the model. We recall that one of the aim of our cortical column model

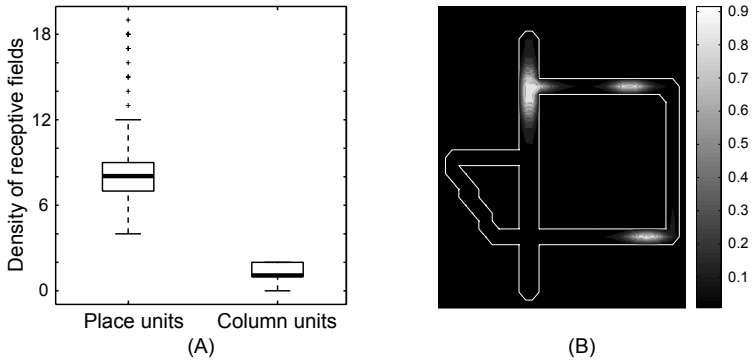

Fig. 5. (A) Spatial density (i.e., mean number of units selective for a place) of the receptive fields of HP cells and cortical column units. **(B)** Samples of receptive fields of three column units.

was to build a less redundant state-space representation, compared to the HP field representation. Fig. 5A shows that the cortical network permitted to reduce the redundancy of the learnt spatial map significantly, compared to the upstream hippocampal space code (ANOVA, $F_{1,316} = 739.2$, $p < 0.0001$). Finally, Fig. 5B displays some samples of cortical column receptive fields of the model.

4 Discussion

We presented a navigation model based on the columnar organisation of the mammalian cortex. It builds a topological map of the environment incrementally, and it uses it to plan an efficient course of actions leading to a goal location. The model was successfully employed to solve the classical Tolman & Honzik's behavioural task [12]. As aforementioned, other models have been proposed to solve goal-directed navigation tasks. They are mainly based on the properties of hippocampal (e.g., Samsonovich and Ascoli 2005, [19]), and prefrontal cortex (e.g., Hasselmo 2005, [7]) neural assemblies. However, most of these models do not perform action *planning* as defined in this paper (see Sec. 1). Samsonovich and Ascoli [19] rather implements a local path finding mechanism to select the most suitable orientation leading to the goal. Similarly, Hasselmo's model [7] do not plan a sequence of actions from the current location s to the goal s_g but only infers the first local action to be taken, based upon a back-propagated goal signal. Yet, these two models rely on discretized state spaces (where predefined grid units code for places), whereas our model uses a distributed population of HP cells providing a continuous representation of the environment [16]. Also, our model learns topological maps coding for the state-action space $S \times A$ simultaneously. In the model by Samsonovich and Ascoli (2005) no topological information is represented, but only a distance measure between each visited place and a set of potential goals. Likewise, in Hasselmo's model states and actions are not jointly represented, which generates a route-based rather than a map-based navigation system [20].

The preliminary version of the model enabled us to investigate some basic computational properties, such as the ability of the columnar organisation to learn a compact state-space representation encoding topological information, and the efficiency of the

activation-diffusion planning mechanism. Further efforts will be put to extend the current model to integrate multiple sources of information. For example, the animat should be able to learn maps that encode all the reward (subjective) values, and action-cost constraints. Also, these maps should be suitable to represent multiple spatio-temporal scales to overcome the intrinsic limitation of the activation-diffusion mechanism in large scale environments. Additionally, these multiscale maps should allow the model to infer high-level shortcuts to bypass the low-level constraints of the environment.

To conclude, although the model has been based upon biological knowledge, some of our working hypotheses are still under debate. First, the existence of cortical columns has been questioned recently [21]. Second, the hippocampus has also been proposed as a likely brain structure encoding topological maps [22]. Yet, the HP cell representation seems too redundant and distributed to constitute a suitable substrate for compact topological map learning [23]. Also, the evidence for high-level spatial representations mediated by neocortical areas (such as the prefrontal cortex, PFC [24]) corroborates the hypothesis of an action planning processing shared among multiple cortical regions [25]. In particular, several experimental observations [24, 26] point towards a role of the PFC in abstract map building and action selection.

Acknowledgments. Funded by the EC Integrated Project ICEA, IST-027819-IP.

References

1. Meyer, J.A., Filliat, D. Cogn Syst Res **4**(4) (2003) 283–317
2. Mountcastle, V.B. J Neurophysiol **20**(4) (1957) 408–34
3. Buxhoeveden, D.P., Casanova, M.F. Brain **125**(5) (2002) 935–51
4. Burnod, Y.: An adaptative neural network: the cerebral cortex. Masson (1989)
5. Bieszczad, A. Proc World Congr Comput Intell WCCI94 **3** (1994) 1313–18
6. Frezza-Buet, H., Alexandre, F. In: IEEE Int Jt Conf Neural Netw. Volume 1. (1999) 252–57
7. Hasselmo, M.E. J Cogn Neurosci **17**(7) (2005) 1115–29
8. Schmajuk, N.A., Thieme, A.D. Biol Cybern **67**(2) (1992) 165–74
9. Dehaene, S., Changeux, J.P. Proc Natl Acad Sci U S A **94**(24) (1997) 13293–98
10. Banquet, J.P. *et al.* Neural Comput **17** (2005) 1339–84
11. Fleuret, F., Brunet, E. Neural Computation **12**(9) (2000) 1987–2008
12. Tolman, E.C., Honzik, C.H. Univ Calif Publ Psychol **4**(14) (1930) 215–32
13. O'Keefe, J., Nadel, L.: The Hippocampus as a Cognitive Map. Oxford Univ Press. (1978)
14. Wiener, S.I., Taube, J.S.: Head Direction Cells and the Neural Mechansims of Spatial Orientation. MIT Press (2005)
15. Arleo, A., Gerstner, W. Neurocomputing **38**(40) (2001) 1059–65
16. Arleo, A., Smeraldi, F., Gerstner, W. IEEE Trans Neural Netw **15**(3) (2004) 639–51
17. Rao, S.G., Williams, G.V., Goldman-Rakic, P.S. J Neurophysiol **81**(4) (1999) 1903–16
18. Triesch, J. Neural Comput **19**(4) (2007) 885–909
19. Samsonovich, A., Ascoli, G. Learn Mem **12** (2005) 193–208
20. Arleo, A., Rondi-Reig, L. J Integr Neurosci **6**(3) (2007) 327–66
21. Horton, J.C., Adams, D.L. Philos Trans R Soc Lond B Biol Sci **360**(1456) (2005) 837–862
22. Poucet, B. *et al.* Rev Neurosci **15**(2) (2004) 89–107
23. Wilson, M.A., McNaughton, B.L. Science **261** (1993) 1055–58
24. Hok, V. *et al.* Proc Natl Acad Sci U S A **102**(12) (2005) 4602–07
25. Knierim, J.J. Learn Mem **13**(4) (2006) 405–15
26. Granon, S., Poucet, B. Behav Neurosci **109**(3) (1995) 474–84